https://doi.org/10.15407/ujpe70.6.406

D. FEDONENKO,[1] S.I. PETRUSHENKO,[2,3] K. ADACH,[2] M. FIJALKOWSKI,[2] Y.M. SHEPOTKO,[1] S.V. DUKAROV,[3] R.V. SUKHOV,[3] A.L. KHRYPUNOVA,[1] N.P. KLOCHKO[1]

[1] National Technical University "Kharkiv Polytechnic Institute"
(2, Kyrpychova Str., Kharkiv 61002, Ukraine; emails: denis.fedonenko@gmail.com, j4cksons123@gmail.com, khrip@ukr.net, klochko.np16@gmail.com)

[2] Technical University of Liberec
(2, Studentska Str., Liberec, 46117, Czech Republic; emails: Serhii.Petrushenko@tul.cz, kinga.adach@tul.cz, mateusz.fijalkowski@tul.cz)

[3] V.N. Karazin Kharkiv National University
(4, Svobody Square, Kharkiv 61022, Ukraine; emails: s.dukarov@karazin.ua, sukhov@karazin.ua)

NANOSTRUCTURED COPPER IODIDE FILM IN A MULTIFUNCTIONAL FLEXIBLE DEVICE FOR ULTRAVIOLET PHOTODETECTION AND AMMONIA MONITORING

A flexible, lightweight, and portable device integrating the functions of an ammonia gas sensor and an ultraviolet (UV) photodetector operating at room temperature is developed using available materials with no physiological toxicity and low manufacturing cost by employing the low-temperature aqueous successive ionic layer adsorption and reaction (SILAR) method to deposit a nanostructured copper iodide (CuI) thin film on a flexible polyethylene (PE) substrate. Under the irradiation of UV radiation, it functions as a flexible photoconductive UV photodetector with a photoconductivity gain of 1.17, a sensitivity of 2.3 mA/W, a specific detectivity of 1×10^9 Jones and an external quantum efficiency of 0.8% with a response/recovery time of several minutes. It is quite suitable for wearable personal UV monitoring devices and as an electronic eye in door security system. The high selective sensitivity of the device to ammonia (NH_3) is due to the synergistic effect of the electron donor gas NH_3 on the p-type semiconductor CuI and its ability to complexing NH_3. The detection limit of 0.15 ppm of the CuI/PE chemiresistive ammonia sensor and its fast response/recovery make it suitable for food spoilage detection, real-time monitoring of ammonia leaks, and in medical diagnosis by detecting NH_3 in exhaled air.

Keywords: UV detectors, chemical detectors, flexible substrates, thin films, CuI, nanocrystalline layers.

1. Introduction

Among the Sustainable Development Goals (SDG_s) presented in the 2030 Agenda for Sustainable Development, Goal 9 aims to build sustainable infrastructure, promote sustainable industrialization and stimulate innovation. In order to diversify the industry and increase the value addition to commodities by creating new products without polluting the environment and, at the same time, expanding scien-

Citation: Fedonenko D., Petrushenko S.I., Adach K., Fijalkowski M., Shepotko Y.M., Dukarov S.V., Sukhov V.M., Khrypunova A.L., Klochko N.P. Nanostructured copper iodide film in a multifunctional flexible device for ultraviolet photodetection and ammonia monitoring. *Ukr. J. Phys.* **70**, No. 6, 406 (2025). https://doi.org/10.15407/ujpe70.6.406.

tific research, a promising approach is to use easy-to-manufacture technologies and widely available nontoxic and biocompatible materials to produce innovative, affordable and low-cost micro- and nanoelectronic devices. As a part of sustainable technologies, flexible photodetectors for detecting hazardous levels of ultraviolet (UV) light, as well as toxic gas sensors, are important instruments for environmental engineering to protect human health and to improve people's environmental quality of life. These devices have many applications in everyday life, especially if they are based on simple and inexpensive solution manufacturing technologies and the use of environmentally friendly materials [1–4]. For example, a promising direction is the development of flexible wearable sensors capable of monitoring ultraviolet radiation and ammonia (NH_3) air pollution [5–9]. The development of a flexible and skin-like ultraviolet photodetector (PD) is particularly important for monitoring UV radiation and protecting people from eye and skin health risks. According to [1–3], flexible UV PDs have attracted extensive research interest due to their potential applications in large-scale optoelectronic devices for personal UV monitoring, UV electronic eye, anti-UV gloves, and other wearable systems. Ammonia is a fatal, colorless, irritating, toxic and flammable air pollutant primarily emitted by chemical plants, farms, and vehicles. According to the Occupational Safety and Health Administration (OSHA) [5, 7], the permissible human exposure limit is 25 ppm NH_3 for 8 hours, and inhaling ammonia gas over an extended period can cause serious breathing problems, permanent heart damage, and various illnesses. This is especially dangerous for people with pre-existing conditions such as asthma or other lung diseases, as they may be at increased risk of more serious complications from ammonia exposure [7]. So, it is critical to develop ammonia detection devices using low-cost, practical and effective technology, As their ability to monitor ammonia leaks in real time allows for early intervention, reducing the risk of accidents, injuries and adverse environmental impacts. On the other hand, ammonia in exhaled gas is important as a marker for medical diagnosis, and typical ammonia concentrations of 0.425–1.8 ppm in exhaled gas have been reported [7, 8]. In particular, it is known [8, 9] that NH_3 at a level below 1 ppm is a medical biomarker of kidney diseases and stomach infections caused by Helicobacter pylori; so, its detection is of great importance for medical diagnostics. Furthermore, ammonia serves as an important marker gas produced by the decomposition of protein-rich foods [7] and can play a key role in detecting food spoilage, since dried aquatic products including meat products, fish, and shrimp will smell like ammonia due to the continuous decomposition of food protein by microorganisms [5, 7, 8]. Thus, flexible wearable and portable gas sensors and ultraviolet photodetectors, which have high mechanical strength and low weight, and do not require heating, since they operate at room temperature, find application in various fields including health monitoring, food safety and environmental protection. Nanostructured thin films of wide-bandgap semiconductors are especially popular among various functional materials of the above-mentioned UV photodetectors of photoconductive and photovoltaic types [2–4, 10–13, 15–17] and chemiresistive NH_3 sensors [2–4, 10–13, 15–17]. Examples include UV photoconductive photodetectors based on nanocrystalline films of zinc oxide (ZnO) [3], tin-doped zinc oxide [4], and copper iodide (CuI) [15]. In these UV PDs, the semiconductor layer illuminated with UV light absorbed the light energy, resulting in the creation of electron-hole pairs and, thus, a large number of photogenerated carriers that formed a photocurrent ($I_{\rm ph}$), when an external bias voltage (U) was applied between the two ohmic electrodes. In the absence of UV radiation, the current decreases exponentially and reaches a minimum value of dark current ($I_{\rm dark}$). In chemiresistive NH_3 sensors, a change in the resistance of the sensing elements depends on the type of semiconductor materials used as sensing elements [14, 20, 21]. According to [20, 21], the gas detection mechanism in the gas sensor is a two-stage process. In the first step, oxygen from the air is adsorbed by the nanostructured sensing surface of the semiconductor. The adsorbed oxygen molecules are then ionized by capturing electrons from the conduction band of n-ZnO [20] or by extracting electrons from the valence band of a p-type semiconductor such as nickel oxide (NiO) or CuI [21], according to the reaction:

$$O_2 + e^- \rightarrow O_2^-. \quad (1)$$

As a result, an electron depletion layer appears on the n-ZnO surface, and the electrical resistance of the zinc oxide surface, whose electrons are held by oxygen ions in the conduction band, increases [20]. On

the contrary, in the p-type semiconductor, the adsorption of atmospheric oxygen leads to a decrease in resistance, since a hole accumulation zone is formed over its entire surface [21]. In the second stage, the electron-donating NH_3 gas molecules, being adsorbed on the semiconductor surface, react with oxygen ions O_2^-, as a result, the electrons are released back into the conduction band of n-ZnO [20] or into the valence band of the p-type semiconductor [21]. Therefore, under the influence of ammonia, the electrical resistance on the zinc oxide surface decreases. The reaction of NH_3 gas detection by the ZnO gas sensor [20] is as follows:

$$4NH_3 + 3O_2^- \rightarrow 2N_2 + 6H_2O + 3e^-. \quad (2)$$

When NH_3 interacts with a nanostructured p-type semiconductor material, the hole concentration in its surface layer decreases due to the injection of electrons into the semiconductor as a result of the oxidation of ammonia by negative species of oxygen O_2^-, which leads to an increase in the resistance of the p-type semiconductor, according to the following reaction [21]:

$$2NH_3 + 3O_2^- \rightarrow NO_2 + NO + 3H_2O + 3e^-. \quad (3)$$

When the atmosphere is changed back to air after the chemiresistive gas sensor has been exposed to NH_3, the resistance is observed to return to its original value. The responses of semiconductor layers to gases in chemoresistive sensors are measured by the currents arising between two ohmic electrodes connected to wide-bandgap semiconductor films when an external electrical voltage U is applied. Similar gas detection mechanisms are typical of many electron donor gases and vapors, including ethanol, acetone, water and other interfering compounds for NH_3 gas analysis using chemiresistive gas sensors based on wide bandgap semiconductor layers [14, 20, 21]. The selectivity and high sensitivity of the determination of ammonia by CuI [19] and other copper compounds with the oxidation state Cu^+, for example, CuBr [18], lies in their ability to bind NH_3 at form temperature, forming the complex $[Cu(NH_3)_2]^+$. According to [22–24], the $[Cu(NH_3)_2]^+$ complex is thermodynamically stable at room temperature. Thus, by injecting electrons, it rapidly and strongly increases the resistance of these p-type semiconductor materials in an atmosphere containing ammonia.

A distinctive feature of CuI, namely its cubic γ-phase, is that copper iodide is a p-type semiconductor with a direct band gap of about 3.0 eV and a high exciton binding energy of 58–62 meV [15, 25–27]. This allows CuI to be used in ultraviolet photodetectors [15–17], which are capable of detecting UV light due to its simultaneous band-to-band and excitonic absorption at room temperature. At the same time, copper iodide, due to the above-mentioned specific complexation reactions with NH_3, as well as because it is a wide-band p-type semiconductor, is a promising candidate for selective and highly sensitive chemiresistive ammonia sensors operating at room temperature [19]. Furthermore, CuI is insoluble in water, unlike copper bromide in the ammonia sensor presented in [18]. Moreover, nanostructured CuI layers with highly hydrophobic surfaces can be prepared using the low-temperature successive ionic layer adsorption and reaction (SILAR) method from widely available materials and have a low environmental impact [26,27]. The biocompatibility of CuI has been demonstrated by its use in antimicrobial dental adhesive systems [28] and as a source of iodine and copper in a dietary food supplement [29]. It is also important that CuI layers can be obtained by the SILAR method on various flexible substrates and with different morphologies [25, 30] to obtain flexible UV photodetectors, as well as bendable ammonia sensors. Since the effect of resistance change is particularly strong in thin nanostructured films with a large specific surface area, morphological changes in nanostructured semiconductor materials have proven to be a controlling factor in the behavior of gas sensors [19, 21] and ultraviolet detectors [2, 10, 11, 13, 15] based on wide-gap semiconductors, including CuI.

Thus, in this work, the effect of the temperature of solutions used in the deposition of copper iodide layers on flexible plastic substrates made of polyethylene (PE) by the SILAR method on the morphology of CuI nanostructures was investigated. Since the main limitation of flexible polyethylene substrates is their low surface energy, which can lead to delamination of the sensitive layer [31], we, in accordance with [32], used plasma modification of the PE surface before CuI deposition in order to increase the wettability of PE to improve the adhesion of CuI to PE. We also investigated the effect of oxidative air-plasma treatment of the PE surface on the morphology of CuI in CuI/PE samples. Then, by equipping

the CuI/PE samples with thin-film ohmic electrodes, we constructed a multifunctional flexible device for ultraviolet photodetection and ammonia monitoring, which combines functions of flexible photoconductive-type UV photodetector and a chemiresistive ammonia gas sensor, and investigated its output characteristics.

2. Materials and Methods

2.1. Materials

Aqueous 25% ammonium hydroxide solution (5.0 M NH_4OH) was purchased from Fluka Chemicals Ltd, UK. Copper(II) sulfate pentahydrate ($CuSO_4{\cdot}5H_2O$), sodium thiosulfate pentahydrate ($Na_2S_2O_3\ 5H_2O$) and sodium iodide (NaI) were purchased from VWR PDH Chemicals, USA. Polyethylene $(C_2H_4)_n$ film of 50 μm thickness (PE) was obtained from Jinjiang Hc Industry Co., Ltd, China.

2.2. Development of a multifunctional flexible device for ultraviolet photodetection and ammonia monitoring

Pieces of flexible polyethylene films with dimensions of 50 × 25 mm were successively cleaned in an ultrasonic bath with isopropanol and distilled water at a temperature of 50 °C for 25 min each. They were used as PE substrates, some of which were directly coated with a copper iodide film using the SILAR method, and other PE substrates were pre-treated with oxidizing air-plasma at atmospheric pressure in accordance with that described in [32]. For this purpose, the discharge was excited at a frequency of 50 kHz using a home-made plasma source, the nozzle of which was located at a distance of 10 cm from the PE surface. The plasma-forming gas flow rate was 30 l/min at an electric power of 685–695 W, the duration of plasma treatment was 1 min. The efficiency of this plasma treatment was tested experimentally by improving the wettability of PE. The reverse side of the PE substrate was then laminated with a self-adhesive polypropylene film, which was removed after the copper iodide layer was applied, so that, in the subsequently obtained CuI/PE samples, the nanostructured copper iodide film was located only on one side of the substrate.

Deposition of nanostructured CuI films on the PE substrates was performed using the automatic SILAR technology using a universal motorized platform with numerical control for commercial 3D printers. Automation of all SILAR steps was programmed using g-code, ensuring reproducibility of the substrate immersion rate and the time of each SILAR step with an accuracy of <0.1%, similarly to that described in [33]. The temperature of all solutions used in the SILAR deposition was controlled at 20 °C or 30 °C. During the deposition of the CuI layer, one SILAR cycle consisted of four steps with rapid (0.5 s) immersion of the substrate into and out of the solutions. The first step involved immersion of the substrate for 20 s in a cationic aqueous solution containing 0.1 M $CuSO_4$ and 0.1 M $Na_2S_2O_3$, in which the $S_2O_3^{2-}$-ion reduced Cu^{2+} to Cu^+ and also acted as a ligand. The second stage was immersion in distilled water for 50 s to remove weakly adsorbed particles from the surface. The third stage was immersion of the substrate with strongly adsorbed Cu^+-ions for 20 s in an aqueous anionic solution of 0.1 M NaI to obtain a CuI monolayer as a result of the interaction of Cu^+ and I^-. The fourth stage was rinsing in distilled water for 50 s to remove excess ions and weakly bound particles from the surface. After every 10 SILAR cycles, the contaminated distilled water in the washing glasses was replaced with fresh distilled water. After 60 SILAR cycles, CuI/PE samples with a thickness of nanostructured copper iodide films of ∼1 μm, estimated using scanning electron microscopy, were obtained. Two thin-film Au80Pd20 ohmic contacts were deposited by RF magnetron sputtering of an Au80Pd20 target. These thin-film Au80Pd20 contacts were partially covered with self-adhesive aluminum tapes for connection to an external electrical circuit.

2.3. Materials

For morphological characterization and chemical analysis of CuI/PE samples, scanning electron microscopy/energy dispersive X-ray spectrometry (SEM-EDS) analysis was performed using a Zeiss ULTRA Plus SEM with secondary electron (SE) detector equipped with an OXFORD X-Max 20 EDS detector providing elemental mapping. SEM images and EDS spectra were recorded from areas of about 50×50 μm at an accelerating voltage of 2 kV, 5 kV or 10 kV. EDS maps of the samples were superpositions of the signal obtained from the electron backscatter detector (colored white) and the intensities of the characteristic lines of Cu, S, and I (colored in

shades of the corresponding colors). The resolution of the EDS maps was 500 × 500 pixels. Optical diffuse reflectance spectrum $R_d(\lambda)$ of the CuI/PE sample was recorded in the wavelength range λ from 400 to 1100 nm using a LAMBDA 35 PerkinElmer spectrophotometer. The optical band gap E_g for direct allowed transitions in nanostructured CuI film was determined from the $R_d(\lambda)$ spectrum, according to [25, 34, 35], using the Kubelka–Munk function F, calculated using the following equation:

$$F = (1 - R_d)^2/2R_d. \quad (4)$$

According to [25, 34, 35], the E_g value was obtained graphically from the dependence of $(F \cdot h\nu)^2$ on $h\nu$ by extrapolating its linear part to $h\nu$.

In accordance with [36, 37], to analyze the luminescent characteristics of the CuI film, the photoluminescence (PL) spectrum of the CuI/PE sample was excited by 365 nm UV light at room temperature and recorded with a BLACK-Comet CXR-SR-25 fiber optic spectrometer.

2.4. Sensing Measurements

To test the possibility of using the nanostructured copper iodide film in a multifunctional flexible device for ultraviolet photodetection and ammonia control, an experimental sensor prototype was created. For this purpose, two parallel thin-film Au80Pd20 contacts were applied at a distance of 1 cm from each other onto the surface of a copper iodide film deposited by the SILAR method onto a plasma-treated polyethylene tape at a solution temperature of 30 °C using a shadow mask by the RF magnetron sputtering method. Then the Au80Pd20 thin-film contacts were partially covered with self-adhesive aluminum tapes for their connection to an external electric circuit. The resulting flexible device, which we named CuI/PE, was then tested as a metal-semiconductor-metal (MSM) ultraviolet photodetector and as a chemiresistive ammonia gas sensor.

2.4.1. Testing of CuI/PE UV photodetector with MSM structure

For the UV illumination, a PHILIPS TL 6W/08 BLB G5 T5.226.3M ultraviolet lamp with an average wavelength of 367 nm and a P_{light} intensity of 1.17 mW/cm^2 was used. Current-voltage ($I-U$) and current-time (I-t) characteristics were measured using a GW Instek LCR-6002 meter in the dark and under UV light. The effective irradiation area of the UV photodetector $A = 0.1$ cm^2 was limited by a screen with a slit 1 mm wide. To evaluate the performance of the experimental prototype of the flexible CuI/PE UV PD, a bias voltage of $U = 1$ V was applied and the currents in the dark (I_{dark}) and under UV illumination (I_{light}) were simultaneously recorded in air at room temperature. The output characteristics of the photodetector were calculated in accordance with the formulas given in [3, 10, 11, 13, 15, 38] and analyzed with regard for the information presented in [39–41].

2.4.2. Test of CuI/PE chemiresistive ammonia gas sensor

An experimental prototype of the CuI/PE sensor was tested as a flexible chemiresistive sensor for determining the ammonia content in air at room temperature using a test setup with a 1.7-liter glass test chamber. To test the CuI/PE gas sensor, a 5.0 M NH_4OH liquid solution was introduced, similar to that described in [27], through a microdosing syringe-microdispenser into the chamber, where it quickly evaporated. The chamber remained sealed throughout the test. The resistance value of the CuI/PE sample inside the test chamber immediately before the introduction of ammonia was determined as R_0. It was measured between the Au80Pd20 thin-film contacts by determining the current at a voltage U between the contacts of 1 V. The increase in resistance from R_0 to R_g for the CuI/PE sensor under the influence of 0.15–3.0 ppm NH_3 in air was continuously monitored by a GW Instek LCR-6002 meter and visualized on the monitor screen as dynamic response curve ($R - t$). In addition, resistance measurements were performed using a UNI-T UT171C RMS digital multimeter. According to [14], the response time (t_{responce}) was defined as the time required for the sensor to reach 90% of the maximum resistance value R_g. The chamber was then purged with clean dry air using an air compressor and the recovery curve was recorded as the drop in sensor resistance over time from R_g to R_0. According to [14], the recovery time (t_{recovery}) was defined as the time required for the maximum value to decrease to 10% of R_g. To assess the sensitivity of the CuI/PE chemiresistive sensor at

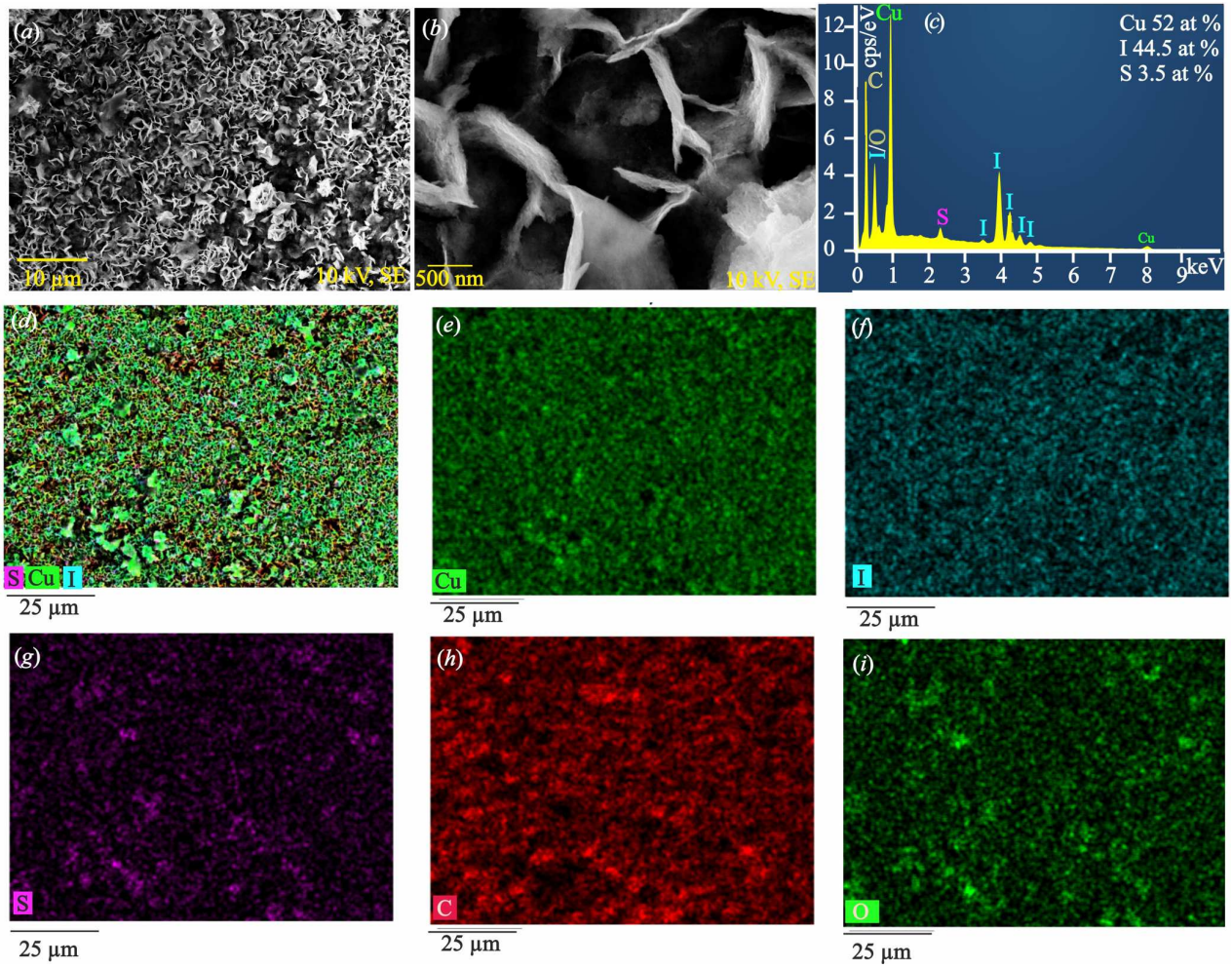

Fig. 1. SEM images obtained at low (*a*) and high (*b*) magnification for a nanostructured copper iodide film with nanoflake morphology deposited on a non-plasma treated polyethylene substrate using the automatic SILAR method at solution temperatures of 20 °C. EDS spectrum of this CuI/PE sample (*c*). Overall EDS map of this CuI/PE sample (*d*). Elemental EDS mapping of individual elements in this CuI/PE sample: Cu (*e*); I (*f*); S (*g*); C (*h*); O (*i*)

room operating temperature, its response S to ammonia was determined according to [6, 14, 20, 31] using the formula:

$$S^* = (R_g - R_0)/R_0 = \Delta R/R_0. \quad (5)$$

3. Results and Discussion

Figures 1, *a*, *b* show the SEM images of the copper iodide nanoflake array deposited on the PE substrate using the automatic SILAR method at solution temperatures of 20 °C. This nanostructured CuI film is similar to those presented in [42] and, according to [43], belongs to an exotic two-dimensional copper iodide material with zinc blende structure γ-CuI. The EDS spectrum of this sample in Fig. 1, *c* and the EDS maps in Figs. 1, *d*, *e*, *f*, *g*, *h*, and *i* shows that the CuI film with nanoflake morphology contains 52 at.% Cu, 44.5 at.% I, and 3.5 at.% S. CuI films obtained by the SILAR method [25, 30] are characterized by the presence of sulfur impurity, caused by partial decomposition of thiosulfate ion in the cationic solution. The EDS maps in Figs. 1, *d*, *e*, *g* and *h* confirm the uniform distribution of these elements in the copper iodide film. The elements C and O in the EDS spectrum of CuI/PE in Fig. 1, *c* and in the EDS maps in Fig. 1, *h*

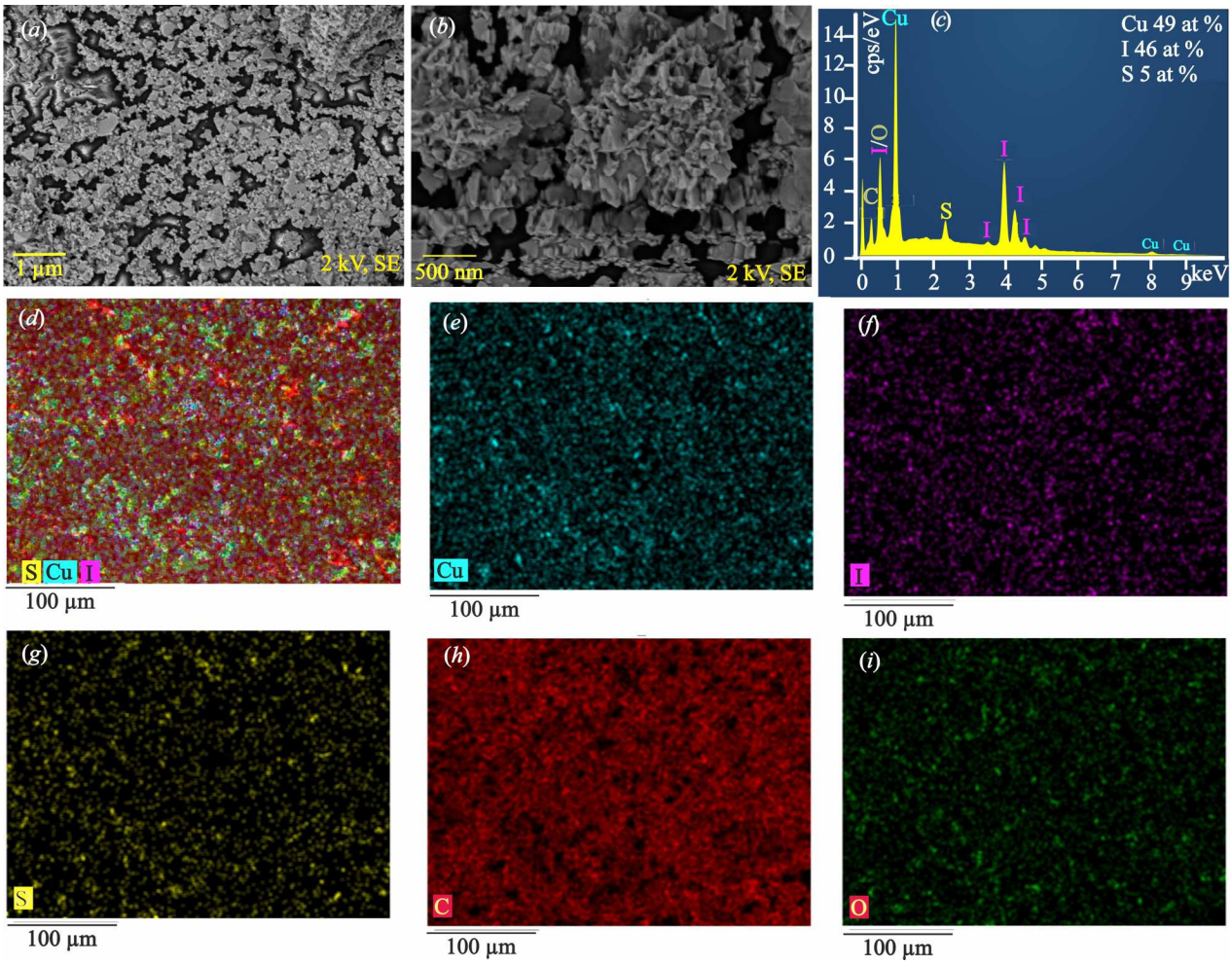

Fig. 2. SEM images obtained at low (*a*) and high (*b*) magnification for a nanostructured copper iodide film deposited on a non-plasma treated polyethylene substrate using the automatic SILAR method at solution temperatures of 30 °C. EDS spectrum of this CuI/PE sample (*c*). Overall EDS map of this CuI/PE sample (*d*). Elemental EDS mapping of individual elements in this CuI/PE sample: Cu (*e*); I (*f*); S (*g*); C (*h*); O (*i*)

and *i* belong to the polyethylene substrate. In order to create a more densely packed structure of the CuI thin film, in which copper iodide crystals form a triangular nanostructure, which, according to literature data [44], allows electrons and holes to move freely without overcoming large distances, the temperature of the solutions used in the deposition via SILAR was increased to 30 °C.

The morphology of the obtained CuI/PE sample, shown in the SEM images in Figs. 2, *a*, *b*, exhibits well-defined triangular-shaped copper iodide nanocrystals. The EDS spectrum in Fig. 2, *c* confirms that this CuI film is also copper-rich and contains sulfur. At the same time, as can be seen in these SEM images, as well as in the overall EDS map in Fig. 2, *d*, the CuI film covers the surface of the polyethylene substrate unevenly and incompletely due to the low wettability of PE [31], which causes poor adhesion to the PE of the CuI layer applied in aqueous solutions using the SILAR method.

Fig. 3 shows photos of water droplets on the PE surface before (*a*) and after (*b*) plasma modification, which increased the hydrophilicity of the polyethylene substrate. The effect of oxidative air-plasma treatment of the PE surface on the morphology of CuI in a CuI/PE sample obtained on such a polyethy-

lene substrate by the SILAR method using solutions heated to 30 °C is shown in Fig. 4. In the SEM image in Fig. 4, *a*, we see a CuI/PE sample with a nanostructured thin film of copper iodide, the grains of which have a triangular shape with a random orientation in the plane. This morphology is a typical crystal characteristic of the (111)-textured cubic structure of zinc blende γ-CuI, since {111} is the lowest energy surface [36, 44–47], which promotes charge transport [30, 44]. It is also important that the copper iodide film on the plasma-treated polyethylene film completely covers the surface of the substrate. The EDS spectrum in Fig. 4, *b* shows that the CuI in this CuI/PE sample is enriched in iodine and contains sulfur additive. This composition promotes the formation of intrinsic copper vacancy defects V_{Cu}, which form acceptor levels near the valence band, resulting in high p-type conductivity at room temperature [27, 40]. Furthermore, doping with impurity acceptors by replacing iodine with chalcogen impuritiy S to form S_I defects can be a way to further enhance the p-type conductivity of CuI [40, 48, 49]. The overall and elemental EDS maps in Figs. 4, *c, d, e* and (*f*) confirm the homogeneous chemical composition of this CuI/PE sample.

A photo of the CuI/PE sample in Fig. 5, *a* shows a slightly yellowish color of the copper iodide film deposited on the plasma-treated polyethylene substrate using the automatic SILAR method at solutions temperature of 30 °C. According to [40], this color corresponds to the high sub-gap absorption of copper iodide, which is associated with intrinsic defects such as V_{Cu}, iodine vacancies V_I and clusters of defects of V_I and interstitial copper Cu_i. Also, the yellowish color of copper iodide can be associated with S_I defects arising due to the presence of sulfur impurity and/or the defects at grain boundaries [40, 48, 49]. The broad luminescence peak centered at ∼470 nm (i.e., 2.6 eV) observed for this CuI thin film in Fig. 5, *b* is a superposition of several PL peaks. Among them, according to [36, 40, 41], the PL peak observed at 420 nm can be attributed to the emission caused by the recombination of electrons in the conduction band with neutral copper vacancies V_{Cu}. According to [36, 41], the broad PL peak at 675 nm (i.e., 1.8 eV) in Fig. 5, (*b*) is due to iodine vacancies V_I and their complexes with interstitial copper defects (V_I + Cu_i). The contribution of defects associated with sulfur impurity, for example S_I, in the photoluminescence spectrum of copper iodide film in Fig. 5, *b* should also not be excluded. The diffuse reflectance spectrum in Fig. 5, *c* with high R_d throughout the visible and near infrared range corresponds to the rough surface of the nanostructured CuI film deposited on the plasma-treated polyethylene substrate using the automatic SILAR method at solutions temperature of 30 °C. The plot of $(Fhv)^2$ versus hv in Fig. 5, *d*, obtained using the Kubelka–Munk function, determined the band gap for direct optical transitions E_g in the CuI film to be 2.8 eV. This value of E_g is lower than the typical $E_g \approx 3.0$ eV for CuI, as well as for CuI : S films containing 3–5 at.% S in [48]. The reduced band gap of copper iodide in the CuI/PE sample can be explained by the sub-gap absorption due to defects inside the CuI nanocrystals and at their grain boundaries, which is demonstrated in Fig. 5, *d*) as a broad Urbach tail for this nanocrystalline material at energies below 2.8 eV. The same E_g value was obtained for CuI films deposited by the SILAR method in [44].

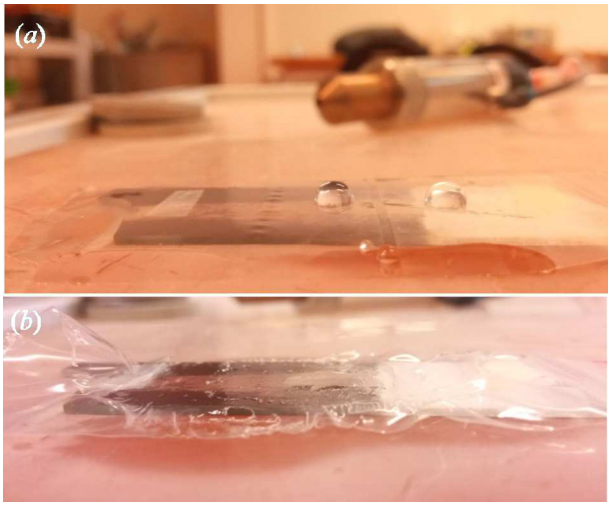

Fig. 3. Photos of PE substrates before (*a*) and after preliminary treatment with an oxidizing air-plasma for 1 min at a gas flow rate of 30 l/min and an electric power of 685–695 W (*b*), demonstrating an improvement in the wettability of the PE. At the top in (*a*) is a homemade plasma source, the nozzle of which was located at a distance of 10 cm from the PE surface during preliminary plasma treatment

Thus, the most promising was selected to be the nanostructured copper iodide film applied to a plasma-treated polyethylene substrate using the automatic SILAR method at solution temperatures of 30 °C. The next task was to analyze the suitability

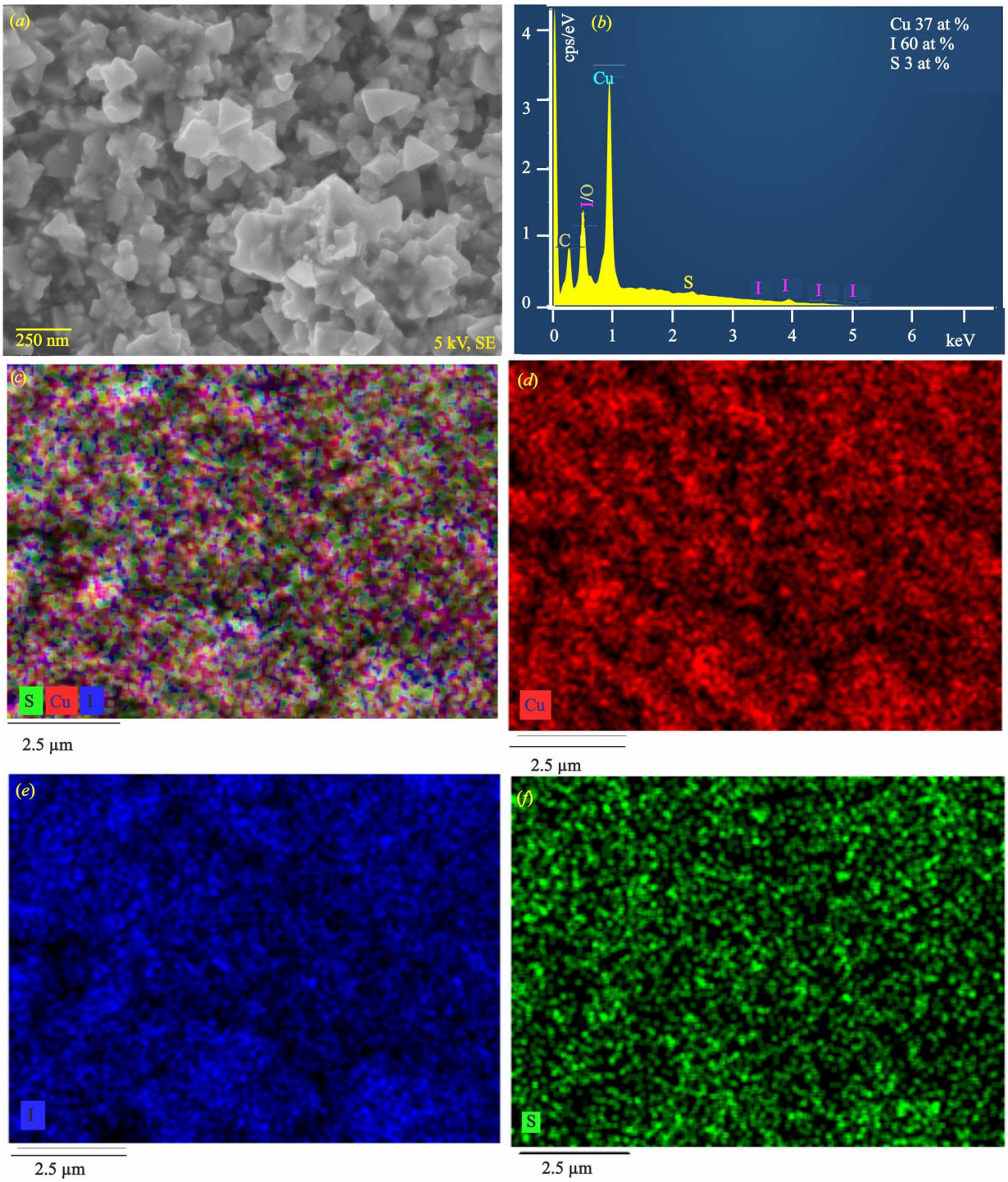

Fig. 4. SEM image of nanostructured copper iodide film with triangle morphology of copper iodide deposited on a plasma treated polyethylene substrate using the automatic SILAR method at the temperature of solutions 30 °C (*a*). EDS spectrum of this CuI/PE sample (*b*). Overall EDS map of this CuI/PE sample (*c*). Elemental EDS mapping of individual elements in this CuI/PE sample: Cu (*d*); I (*e*); S (*f*)

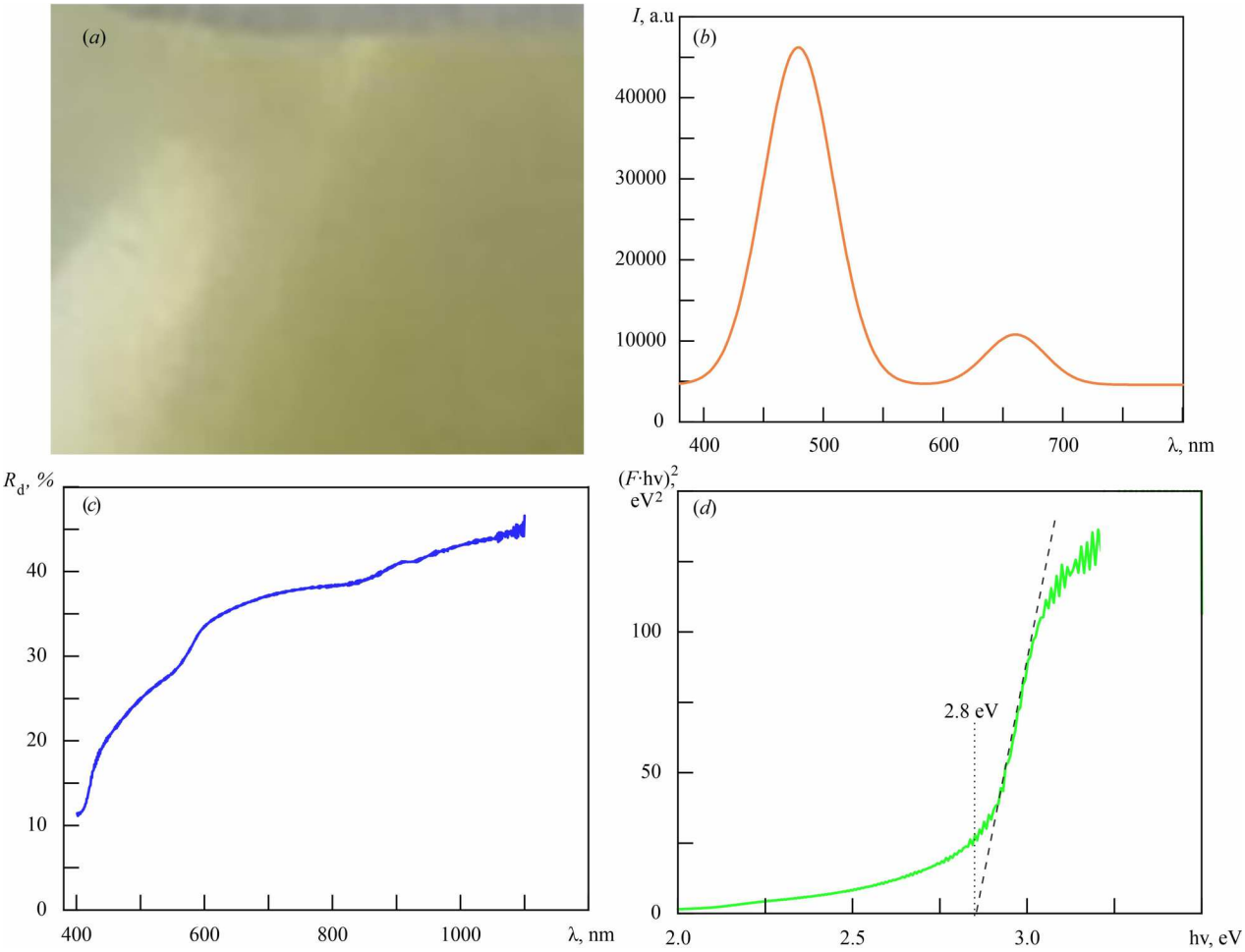

Fig. 5. Photo of CuI/PE sample with nanostructured copper iodide film deposited on a plasma treated polyethylene substrate using the automatic SILAR method at solution temperatures of 30 °C (*a*). PL spectrum of this sample (*b*). Optical diffuse reflectance spectrum $R(\lambda)$ of this sample (*c*). Graph for determining the band gap of the nanostructured CuI film in this sample using the Kubelka–Munk function (*d*)

of the multifunctional flexible CuI/PE device with two parallel Au80Pd20 thin-film contacts developed in this work, a photo of which is shown in Fig. 6, *a*, for use as an ultraviolet photodetector. Figure 6, *b* shows the ultraviolet lamp with an average wavelength of 367 nm and a P_{light} intensity of 1.17 mW/cm^2. Using this lamp, the current-voltage characteristic of the CuI/PE UV photodetector in Fig. 6, *c* and its current-time characteristics in Fig. 6, *d*, demonstrating the dependence of the photocurrent on time at a bias voltage of 1 V, were obtained.

The current-voltage characteristics of the CuI/PE UV photodetector with MSM structure in Fig. 6, *c* in the dark and under UV illumination were found to be symmetrical and linear in both current and voltage, indicating the formation of ohmic contacts at the Au80Pd20-CuI interfaces in the range of applied bias voltage. Similar linear *I-U* characteristics have been demonstrated in the literature for CuI-based [38] and SnO_2-based [50] metal-semiconductor-metal photodetectors.

As can be seen in Fig. 6, *d*, after switching on the UV illumination at a bias of $U = 1$ V, the photogenerated current increased compared to the dark current from $I_{\text{dark}} = 1.63$ μA to $I_{\text{light}} = 1.9$ μ. Thus, the sensitivity of the CuI/PE UV photodetector, defined in accordance with [15, 38] as the photoconductivity gain (G_{ph}), i.e. the ratio of the light current to the

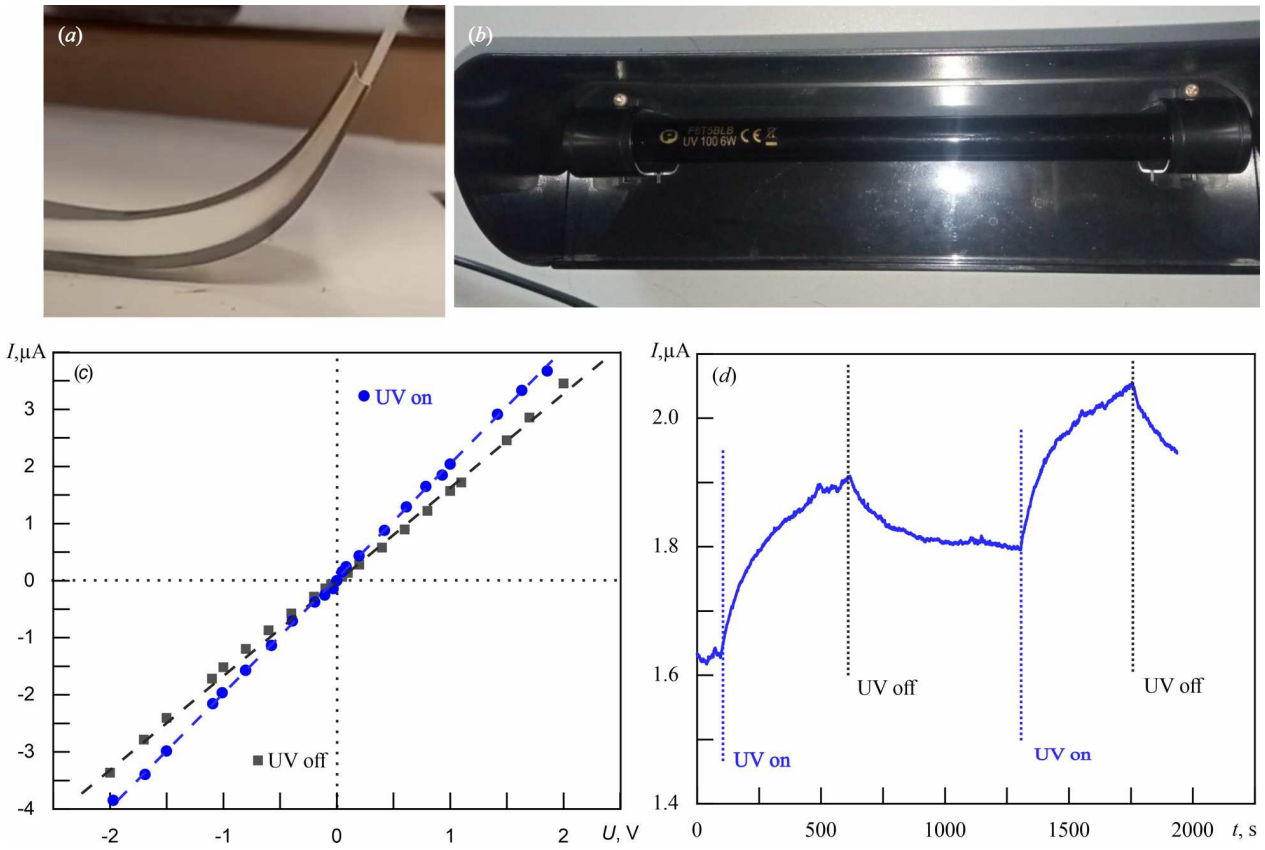

Fig. 6. Photo of the multifunctional flexible CuI/PE device with two parallel Au80Pd20 thin-film contacts (*a*). Photo of the PHILIPS TL 6W/08 BLB G5 T5.226.3M ultraviolet lamp with an average wavelength of 367 nm and a P_{light} intensity of 1.17 mW/cm^2 (*b*). *I-U* characteristics of the CuI/PE ultraviolet photodetector in the dark and under UV illumination with $\lambda = 367$ nm and $P_{\text{light}} = 1.17$ mW/cm^2 (*c*). Current-time characteristics of the CuI/PE UV photodetector at a bias voltage of 1 V when turning on/off UV light with $\lambda = 367$ nm and $P_{\text{light}} = 1.17$ mW/cm^2 (*d*)

dark current expressed as:

$$G_{\text{ph}} = I_{\text{light}}/I_{\text{dark}} \tag{6}$$

at an illumination intensity of $P_{\text{light}} = 1.17$ mW/cm^2 was $G_{\text{ph}} = 1.17$.

The sensitivity to ultraviolet radiation as a responsivity (R_{UV}) of the CuI/PE UV photodetector, which, according to [3, 10, 11, 13, 15, 38], refers to the ratio of the photocurrent generated by the device ($I_{\text{ph}} = I_{\text{light}} - I_{\text{dark}}$) to the incident light power, was defined using the following equation:

$$R_{\text{UV}} = I_{\text{ph}}/P_{\text{light}}A. \tag{7}$$

in which A is the effective irradiation area of this MSM photodetector ($A = 0.1$ cm^2).

The calculation showed $R_{\text{UV}} = 2.3$ mA/W for the experimental sample of the CuI/PE UV photodetector developed in this work at the illumination intensity of 1.17 mW/cm^2 and the bias voltage of 1 V. This R_{UV} value is similar to the sensitivity values obtained for flexible UV photoconductive MSM photodetectors [10], including UV PD based on an array of layered zinc-aluminum double hydroxide nanosheets [2] on a magnetron-sputtered ZnO film [3] and on a wet-chemically deposited CuI film [15]. According to [15], the responsivity can be improved by reducing I_{dark}, for example by replacing ohmic contacts with Schottky barriers.

Considering that the specific detectivity (D^*) is an important parameter of the photodetector, characterizing its signal-to-noise ratio, which is the ability of the photodetector to detect the smallest optical sig-

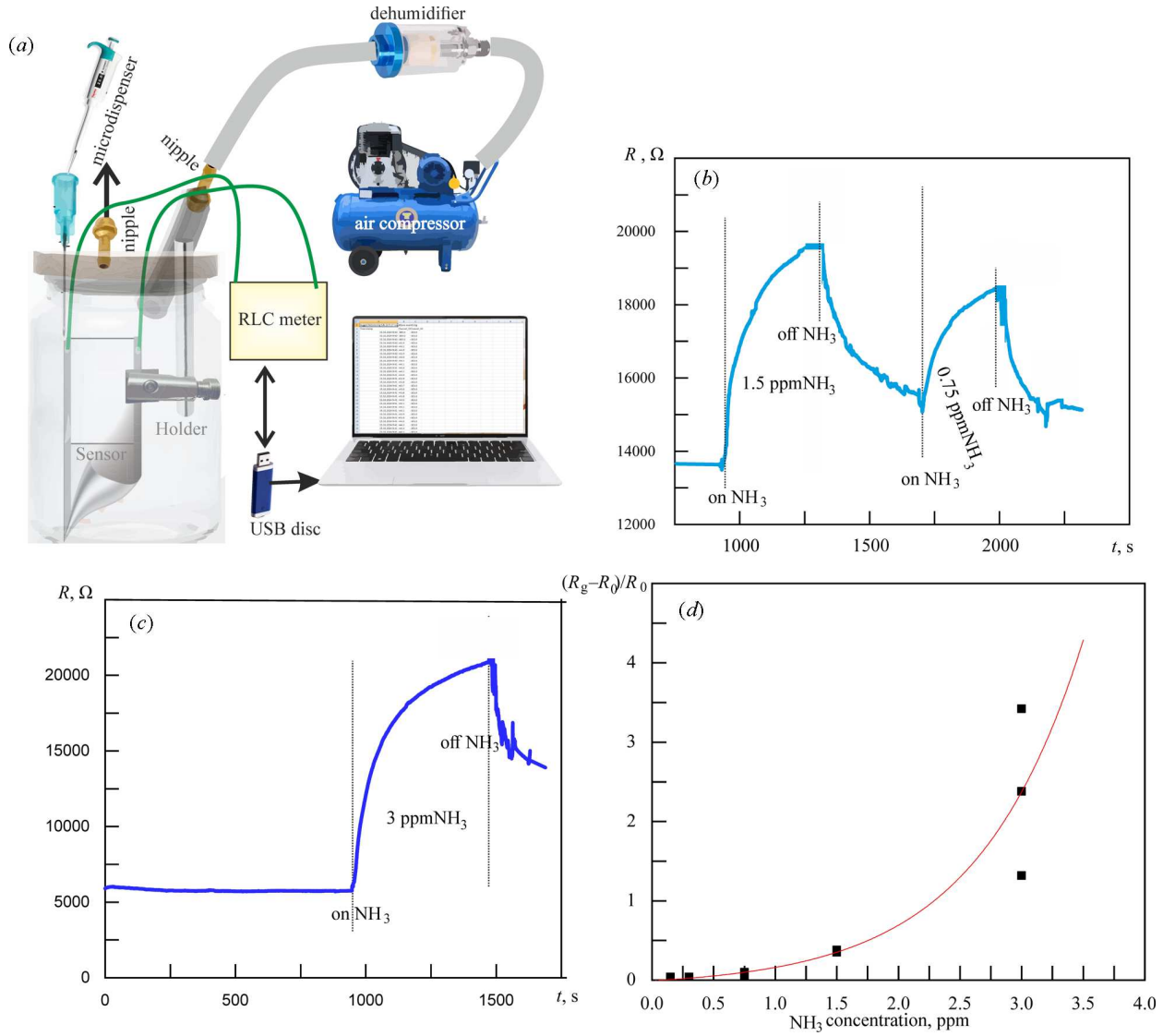

Fig. 7. Schematic representation of the measuring unit of the CuI/PE chemiresistive ammonia sensor (*a*). Response/recovery curves of the CuI/PE chemiresistive ammonia sensor with nanostructured copper iodide film deposited on the plasma-treated polyethylene substrate using the automatic SILAR method at solution temperatures of 30 °C, and two parallel $Au_{80}Pd_20$ thin-film contacts, upon addition to air of 1.5 ppm NH_3 and 0.75 ppm NH3 (*b*) and 3 ppm NH3 (*c*) followed by purging with dry air (bias voltage of 1 V). S^* responses of this ammonia sensor to different NH3 concentrations at room temperature (*d*)

nal [3, 10, 15, 38], it was obtained using the following equation:

$$D^* = R(A/2eI_{\text{dark}})^{1/2}. \tag{8}$$

where e is the electron charge.

According to calculations, the CuI/PE ultraviolet photodetector developed in this work has a relatively large $D^* = 1\times10^9$ Jones (1 Jones = 1 cm $\cdot$ $\text{Hz}^{1/2}$ $\cdot$ W).

In addition, an important parameter of the photodetector is the external quantum efficiency (EQE) which measures the efficiency of converting photons into electrons. EQE is quantitatively defined as the ratio of photogenerated carriers collected by the photodetector electrodes to the number of photons incident on its surface using the equation [3, 15, 38]:

$$EQE = R(hc/e\lambda). \tag{9}$$

where h is Planck's constant, c is the speed of light, and λ is the wavelength of the incident light. The obtained low *EQE* of 0.8% is explained by the nanostructured nature and abundance of defects inside and at the grain boundaries of the CuI film in the CuI/PE UV photodetector. For the same reason, due to the slowdown of charge carrier transfer, the response and recovery time of the CuI/PE UV photodetector is quite long and amounts to several minutes. Nevertheless, in terms of the sum of output parameters, the multifunctional flexible device made in this work from inexpensive, readily available and biocompatible materials is quite suitable for detecting ultraviolet radiation for personal UV monitoring and in wearable applications such as UV electronic eye as a door safety system, anti-UV gloves, *etc.*

The test results of the multifunctional flexible CuI/PE device as a chemiresistive sensor of gaseous ammonia using the measuring unit shown in Fig. 7, *a* are presented in Figs. 7, *b, c, d*. Experiments have revealed the high selective sensitivity of CuI/PE to ammonia in the form of a rapid and strong increase in resistance from R_0 to R_g in an ammonia-containing atmosphere. This sensitivity to ammonia is a synergistic effect of the influence of the electron donor gas NH_3 on the p-type semiconductor, which is the nanostructured copper iodide film deposited by the SILAR method [21, 25, 30], and the ability of CuI to bind NH_3 at room temperature with the formation of the complex $[Cu(NH_3)_2]^+$, according to [18, 21–24]. Similar ammonia sensing results were reported in [19] for copper iodide nanomaterials combined with copper iodide-isopropanolamine complexes. The detection limit (LoD) of the CuI/PE ammonia sensor has been found to be as low as 0.15 ppm, making it suitable for food spoilage detection, real-time monitoring of small ammonia leaks to reduce environmental impacts, and medical diagnostics by detecting ammonia in exhaled gas [5, 7–9]. Fig. 7, *b* and *c* show the fast response/recovery behavior of the CuI/PE sensor to low ammonia concentrations. According to [31, 51, 52], the response time (t_{responce}), defined as the time required for the sensor to reach 90% of the maximum resistance value R_g, is in the range of 250–500 s. After the test chamber is purged with clean dry air using an air compressor and the recovery curve is recorded as a drop in sensor resistance over time from R_g to R_0, the recovery time (t_{recovery}) defined according to [31, 51, 52] as the time required for the maximum value to decrease to 10% of R_g, is up to 700 s.

Figure 7, *d* shows the responses $S^* = \Delta R/R_0$ of the CuI/PE ammonia sensor operating at room temperature to different NH_3 concentrations. According to the data [31, 51, 52], in the region of extremely low concentrations of inorganic gases or organic volatiles, for most sensor materials, a directly proportional dependence of S^* on concentration is not observed. Similarly, Fig. 7, *d* shows the dependence of S^* on ammonia concentration, approximated by an exponential function. The S^* values obtained in this work are higher than those of most modern flexible room-temperature chemiresistive ammonia sensors based on various inorganic and organic nanostructures and their nanocomposites [5–8, 52, 53]. Our results are similar to the S^* data presented in [54] for an ultrasensitive flexible room-temperature ammonia gas sensor based on Au-functionalized polypyrrole-wrapped MoS [2] nanosheets enriched with edge sulfur vacancies. At the same time, the multifunctional flexible CuI/PE device combines excellent ammonia detection properties including high sensitivity, selectivity, reversibility and fast response/recovery at room temperature, while, unlike the sensor in [54], it has no physiological toxicity, is made of readily available materials and has a low manufacturing cost.

Further experiments showed that UV radiation and NH_3 do not interfere with each other, which allows the output signals generated by them to be separated in the multifunctional flexible CuI/PE device.

4. Conclusions

In this work, the flexible, lightweight and portable device that combines the functions of an ammonia gas sensor and a UV photodetector operating at room temperature is presented in the context of developing a manufacturing technology with lower environmental impact, optimizing resource efficiency and creating materials for sustainable development. To do this, we used the low-temperature SILAR method to deposit a thin nanostructured film of the widely available, biocompatible and low-cost material copper iodide. A study of the effect of the temperature of solutions used in the application of copper iodide layers onto flexible polyethylene substrates using the SILAR method on the morphology and chemical composition of CuI, as well as the improvement of the hydrophilicity of the PE surface due to its oxidative air-plasma

treatment, made it possible to optimize the mode for obtaining a CuI/PE sample.Then, by equipping the CuI/PE sample with thin-film ohmic electrodes, we designed a multifunctional flexible device that combines the functions of a flexible photoconductive UV photodetector and a chemiresistive ammonia gas sensor. Under the influence of ultraviolet radiation with an average wavelength of 367 nm and an intensity P_{light} of 1.17 mW/cm^2, its photoconductivity gain $G\text{ph} = 1.17$, sensitivity $R_{\text{UV}} = 2.3$ mA/W, specific detectivity $D^* = 1 \times 10^9$ Jones, external quantum efficiency $EQE = 0.8\%$. The response/recovery time of the CuI/PE UV photodetector is up to several minutes. The performance of the CuI/PE UV PD is attributed to the nanostructured nature and abundant defects inside and at the grain boundaries of the CuI film, which slows down the carrier transport. However, the multifunctional flexible device created in this work is quite suitable for detecting ultraviolet radiation in wearable devices for personal UV monitoring, as well as in electronic eyes in door security systems. The experimentally confirmed high selective sensitivity S^* of the multifunctional flexible CuI/PE device to ammonia is due to the synergistic effect of the action of the electron donor gas NH_3 on the p-type semiconductor, which is the nanostructured copper iodide film, and the ability of CuI to bind NH_3 at room temperature to form the complex $[Cu(NH_3)_2]^+$. The detection limit of 0.15 ppm of the flexible room-temperature CuI/PE ammonia sensor and its fast response/recovery make it suitable for food spoilage detection, real-time monitoring of small ammonia leaks to reduce environmental impact, and medical diagnosis by detecting NH_3 in exhaled breath.

The work was supported by the Ministry of Education and Science of Ukraine and within the MSCA4Ukraine project funded by the European Union. Views and opinions expressed are however, the those of the author(s) only and do not necessarily reflect the views of the European Union. Neither the European Union, nor the MSCA4Ukraine Consortium as a whole, nor individual member institutions of the MSCA4Ukraine Consortium can be held responsible for them.

1. Z-X. Zhang, T. Haggren, J-X. Li, J. Wang, Q-L. Fang, H.H. Tanand, L-B. Luo. High-performance flexible GaAs nanofilm UV photodetectors. *ACS Appl. Nano Mater.* **6** (11), 9917 (2023).
2. A.M. Thomas, C. Yoon, S. Ippili, V. Jella, T.Y. Yang, G. Yoon, S.G. Yoon. High-performance flexible ultraviolet photodetectors based on facilely synthesized ecofriendly ZnAl : LDH nanosheets. *ACS Appl. Mater. Interfaces* **13** (51), 61434 (2021).
3. Y. Li, H. Ma, W. Hu, Y. Zhao. Highly transparent oxide-based ultraviolet photodetectors for flexible electronics. *J. Mater. Sci.: Mater. Electron* **33**, 15546 (2022).
4. M. Vald's, E.A. Villegas, L.A. Ramajo, R. Parra. Ultraviolet-sensor based on tin-doped zinc oxide thin films grown by spray pyrolysis. *Ceramics* **7**, 1500 (2024).
5. S.D. Lawaniya, S. Kumar, Y. Yu, K. Awasthi. Nitrogen-doped carbon nano-onions/polypyrrole nanocomposite based low-cost flexible sensor for room temperature ammonia detection. *Sci. Rep.* **14**, 7904 (2024).
6. J. Cai, C. Zhang, A. Khan, C. Liang, W-D. Li. Highly transparent and flexible polyaniline mesh sensor for chemiresistive sensing of ammonia gas. *RSC Adv* **8**, 5312 (2018).
7. Y. Zhuang, X. Wang, P. Lai, J. Li, L. Chen, Y. Lin, F. Wang. Wireless flexible system for highly sensitive ammonia detection based on polyaniline/carbon nanotubes. *Biosensors* **14**, 191 (2024).
8. C. Zhu, T. Zhou, H. Xia, T. Zhang. Flexible room-temperature ammonia gas sensors based on PANI-MWCNTs/PDMS film for breathing analysis and food safety. *Nanomaterials* **13**, 1158 (2023).
9. M. Matsuguchi, K. Horio, A. Uchida, R. Kakunaka, S. Shiba. A flexible ammonia gas sensor based on a grafted polyaniline grown on a polyethylene terephthalate film. *Sensors* **24**, 3695 (2024).
10. Q. Ye, X. Zhang, R. Yao, D. Luo, X. Liu, W. Zou, C. Guo, Z. Xu, H. Ning, J. Peng. Research and progress of transparent, flexible tin oxide ultraviolet photodetector. *Crystals* **11**, 1479 (2021).
11. H.M.S. Ajmal, F. Khan, N.U. Huda, S. Lee, K. Nam, H.Y. Kim, T-H. Eom, S.D. Kim. High-performance flexible ultraviolet photodetectors with Ni/Cu-Codoped ZnO nanorods grown on PET substrates. *Nanomaterials* **9** (8), 1067 (2019).
12. H. Chen, K. Liu, L. Hu, A.A. Al-Ghamdi, X. Fang. New concept ultraviolet photodetectors. *Materials Today* **18** (9), 493 (2015).
13. J. Ding, P. Zhao, H. Chen, H. Fu. Ultraviolet photodetectors based on wide bandgap semiconductor: A review. *Appl. Phys. A* **130**, 350 (2024).
14. Y.T. Tang, Y. Zhao, H. Liu. Room-temperature semiconductor gas sensors: Challenges and opportunities. *ACS Sens.* **7** (12), 3582 (2022).
15. C.Y. Tsay, Y.C. Chen, H.. Tsai, K.H. Liao. Fabrication and characterization of flexible CuI-based photodetectors on mica substrates by a low-temperature solution process. *Materials* **17** (20), 5011 (2024).
16. A. Liu, H. Zhu, M.G. Kim, J. Kim, Y.Y. Noh. Engineering copper iodide (CuI) for multifunctional p-type transparent semiconductors and conductors. *Adv. Sci.* **8** (14), 2100546 (2021).

17. Y.Z. Liu, T. Zhang, L.Y. Shen, H.S. Wu, N. Wang, F.Z. Wang, X.H. Pan, Z.Z. Ye. Self-powered flexible ultraviolet PDs based on CuI/a-ZTO heterojunction processed at room temperature. *ACS Appl. Mater. Interfaces* **15** (24), 29267 (2023).
18. H-Y. Li, C-S. Lee, D.H. Kim, J-H. Lee. Flexible room-temperature NH_3 sensor for ultrasensitive, selective, and humidity-independent gas detection ACS. *Appl. Mater. Interfaces* **10** (33), 27858 (2018).
19. X. Yang, Q. Ling, Y. Lin, Y. Lv, J. Xi, L. Fu, F. Chen, R. Zhang, S. Zhao. Preparation and ammonia sensing of copper iodide nanomaterials combined with copper iodide-isopropanolamine complexes. *Chem. Select* **9**, e202402808 (2024).
20. B. Aydas, A. Atilgan, A. Ajjaq, S. Acar, M. F. Öktem, A. Yildiz. Flexible NH_3 gas sensors based on ZnO nanostructures deposited on kevlar substrates via hydrothermal method. *Ceramics Intern.* **50**, 32477 (2024).
21. S. Ahmed, S. K. Sinha. Studies on nanomaterial-based p-type semiconductor gas sensors. *Environ Sci. Pollut. Res.* **30**, 24975 (2023).
22. A. Marberger, A.W. Petrov, P. Steiger, M. Elsener, O. Kröcher, M. Nachtegaal, D. Ferri. Time-resolved copper speciation during selective catalytic reduction of NO on Cu-SSZ-13. *Nat. Catal.* **1**, 221 (2018)
23. L. Chen, H. Falsig, T.V.W. Janssens, H. Grönbeck. Activation of oxygen on $(NH_3–Cu-NH_3)+$ in NH_3-SCR over Cu-CHA. *J. Catalysis* **358**, 179 (2018).
24. X. Wang, L. Chen, P.N.R. Vennestrøm, T.V.W. Janssens, J. Jansson, H. Grönbeck, M. Skoglundh. Direct measurement of enthalpy and entropy changes in NH3 promoted O_2 activation over Cu–CHA at low temperature. *Chem. Cat. Chem* **13** (11), 2577 (2021).
25. N.P. Klochko, V.A. Barbash, V.R. Kopach, S.I. Petrushenko, Y.M. Shepotko, O.V. Fijalkowski, K.I. Adach, S.V. Dukarov, V.M. Sukhov, A.L. Khrypunova. Composite fabric with nanocellulose impregnated cotton for eco-friendly thermoelectric textile. *Cellulose* **31**, 5947 (2024).
26. M. Jamshidi, J.M. Gardner. Copper(I) iodide thin films: Deposition methods and hole-transporting performance. *Molecules* **29**, 1723-21 (2024).
27. P. Darnige, Y. Thimont, L. Presmanes, A. Barnabé. Insights into stability, transport, and thermoelectric properties of transparent p-type copper iodide thin films. *J. Mater. Chem. C* **11**, 630-15 (2023).
28. A.S. Mennito, M. Schmidt, A. Lane, A. Kelly, C. Sabatini, W. Renne, Z. Evans. Assessing the antimicrobial properties of copper–iodide doped adhesives in an in vitro caries model: A pilot study Contemp. *Clin. Dent.* **13**, 118 (2022).
29. P. Patnaik. *Handbook of inorganic chemicals* (McGraw-Hill, 2003) [ISBN: 0-07-049439-8].
30. N. Klochko, V. Kopach, S. Petrushenko, E. Shepotko, S. Khrypunova. Copper-enriched nanostructured conductive thermoelectric copper(I) iodide films obtained by chemical solution deposition on flexible substrates. *Ukr. J. Phys.* **69** (2), 115-8 (2024).
31. R.J. Rath, J.O. Herrington, M. Adeel, F. Güder, F. Dehghani, S. Farajikhah. Ammonia detection: A pathway towards potential point-of-care diagnostics. *Biosensors and Bioelectronics* **251**, 116100-16 (2024).
32. M. Lehocky, H. Drnovska, B. Lapcikova, A.M. Barros-Timmons, Trindade, M. Zembala, L. Lapcik. Plasma surface modification of polyethylene. *Colloids and Surfaces A: Physicochem. Eng. Aspects* **222**, 125 (2003).
33. S.I. Petrushenko, M. Fijalkowski, V.R. Kopach, Y.M. Shepotko, K. Adach, S.V. Dukarov, V.M. Sukhov, A. Fedonenko, A.L. Khrypunova, N.P. Klochko. Carbon fabric coated with nanostructured zinc oxide layers for use in triboelectric self-powered touch sensors *J. Mater. Sci.: Mater. in Electron.* **35**, 414-20 (2024).
34. Ł. Haryński, A. Olejnik, K. Grochowska, K. Siuzdak. A facile method for Tauc exponent and corresponding electronic transitions determination in semiconductors directly from UV-Vis spectroscopy data. *Opt. Mater.* **127**, 112205 (2022).
35. M. Patel, A. Chavda, I. Mukhopadhyay, J. Kim, A. Ray. Nanostructured SnS with inherent anisotropic optical properties for high photoactivity. *Nanoscale* **8**, 2293 (2016).
36. Y. Zhang, L. Liu, Z. Wang, Y. Yang, F. Xing. Light-assisted defects migration in cuprous iodide (CuI). *J. Alloys and Compounds* **900**, 163456-8 (2022).
37. M. Xia, M. Gu, X. Liu, B. Liu, S. Huang, C. Ni. Luminescence characteristics of CuI film by iodine annealing. *J. Mater. Sci.: Mater. in Electron.* **7**, 5092 (2015).
38. M. Krishnaiah, A. Kumar, D. Mishra, A.K. Kushwaha, S.H. Jin, J.T. Park. Solution-processed CuI films towards flexible visible-photodetectors: Role of annealing temperature on Cu/I ratio and photodetective properties. *J. Alloys and Compounds* **887**, 161326-12 (2021).
39. C-Y. Tsay, Y-C. Chen, H-M. Tsai, P. Sittimart, T. Yoshitake. The role of Zn substitution in improving the electrical properties of CuI thin films and optoelectronic performance of CuI MSM photodetectors. *Materials* **15**, 8145-12 (2022).
40. Z.H. Li, J.X. He, X.H. Lv, L.F. Chi, K.O. Egbo, M-D. Li, T. Tanaka, Q.X. Guo, K.M. Yu, C.P. Liu. Optoelectronic properties and ultrafast carrier dynamics of copper iodide thin films. *Nature Commun.* **13**, 6346 (2022).
41. S.A. Irimiciuc, S. Chertopalov, M. Buryi, Z. Remeš, M. Vondráček, L. Fekete, M. Novotný, Jan Lancok. Investigations on the CuI thin films production by pulsed laser deposition. *Appl. Surface Sci.* **606**, 154868-9 (2022).
42. X. Li, M. Wan. Morphology and hydrophobicity of micro/nanoscaled cuprous iodide crystal. *Crystal Growth and Design.* **6** (12), 2661 (2006).
43. K. Mustonen, C. Hofer, P. Kotrusz, A. Markevich, M. Hulman, C. Mangler, T. Susi, T.J. Pennycook, K. Hricovini, C. Richter, J.C. Meyer, J. Kotakoski, V. Skákalová. Toward exotic layered materials: 2D cuprous iodide *Adv. Mater.* **34**, 2106922-9 (2022).
44. B. N. Ezealigo, A. C. Nwanya, A. Simo, R.U. Osuji, R. Bucher, M. Maaza, F.I. Ezema. Optical and electrochemical capacitive properties of copper (I) iodide thin film de-

posited by SILAR method. *Arabian J. Chem.* **12** (8), 5380 (2019).

45. J. Li, R. Wang, D. Zhang, Z. Su, H. Li, Y. Yan. Copper iodide (CuI) coating as a self-cleaning adsorbent for highly efficient dye removal. *J. Alloys and Compounds* **774**, 191 (2019).
46. T. Stralka, M. Bar, F. Schöppach, S. Selle, C. Yang, H. von Wenckstern, M. Grundmann. Grain and grain boundary conduction channels in copper iodide thin films. *Phys. Status Solidi A* **220**, 2200883-8 (2023).
47. M. Grundmann, F-L. Schein, M. Lorenz, T. Böntgen, J. Lenzner, H. von Wenckstern. Cuprous iodide: A p-type transparent semiconductor, history, and novel applications. *Phys. Status Solidi (a)* **210** (9), 1671 (2013).
48. A.S. Mirza, M. Pols, W. Soltanpoor, S. Tao, G.H.L.A. Brocks, M. Morales-Masis. The role of sulfur in sulfur-doped copper(I) iodide p-type transparent conductors. *Matter* **6** (12), 4306 (2023).
49. F. Geng, L. Wang, T. Stralka, D. Splith, S. Ruan, J. Yang, L. Yang, G. Gao, L. Xu, M. Lorenz, M. Grundmann, J. Zhu, C. Yang. (111)-Oriented growth and acceptor doping of transparent conductive CuI : S thin films by spin coating and radio frequency-sputtering. *Adv. Eng. Mater.* **25**, 2201666-6 (2023).
50. X. Hou, B. Liu, X. Wang, Z. Wang, Q. Wang, D. Chen, G. Shen. SnO_2-microtube-assembled cloth for fully flexible self-powered photodetector nanosystems. *Nanoscale* **5** (17), 7831 (2013).
51. A. Maity, A.K. Raychaudhuri, B. Ghosh. High sensitivity NH_3 gas sensor with electrical readout made on paper with perovskite halide as sensor. *Material. Sci. Rep.* **9**, 7777-10 (2019).
52. Z. Ren, Y. Shi, T. Song, T. Wang, B. Tang, H. Niu, X. Yu. Flexible low-temperature ammonia gas sensor based on reduced graphene oxide and molybdenum disulfide. *Chemosensors* **9**, 345 (2021).
53. A. Nijkoops, M. Ciocca, S. Krik, A. Douaki, A. Gurusekaran, S. Vasquez, M. Petrelli, M.A.C. Angeli, L. Petti, P. Lugli. Flexible and printed chemiresistive ammonia gas sensors based on carbon nanotube and conjugated polymers: a comparison of response and recovery performance. *IEEE Sensors Lett.* **7** (6), 1 (2023).
54. X. Tian, X. Cui, B. Yao, S. Wang, H. Li, T. Chen, X. Xiao, Y. Wang. Ultrasensitive room-temperature flexible ammonia gas sensor based on Au-functionalized polypyrrole wrapped enriched edge sulfur vacancies MoS2 nanosheets. *Sensors and Actuators: B. Chemical* **395**, 134449 (2023).

Received 11.02.25

Д. Федоненко, С.І. Петрушенко, К. Адач, М. Фіялковський, Ю.М. Шепотько, С.В. Дукаров, Р.В. Сухов, А.Л. Хрипунова, Н.П. Клочко

НАНОСТРУКТУРОВАНА ПЛІВКА ЙОДИДУ МІДІ В БАГАТОФУНКЦІОНАЛЬНОМУ ГНУЧКОМУ ПРИСТРОЇ ДЛЯ УЛЬТРАФІОЛЕТОВОГО ФОТОДЕТЕКТУВАННЯ ТА МОНІТОРИНГУ АМІАКУ

З використанням доступних матеріалів, які не мають фізіологічної токсичності та мають низьку вартість виробництва, та шляхом застосування методу низькотемпературної водної послідовної іонної адсорбції та реакції (SILAR) для нанесення тонкої плівки наноструктурованого йодиду міді (CuI) на гнучку поліетиленову (ПЕ) підкладинку створено гнучкий, легкий та портативний пристрій, що поєднує функції датчика газоподібного аміаку та ультрафіолетового (УФ) фотодетектора, який працює за кімнатної температури. Під впливом УФ випромінювання він функціонує як гнучкий фотопровідний УФ фотодетектор з коефіцієнтом фотопровідності 1,17; чутливістю 2,3 мА/Вт; питомою детектувальною здатністю $1 \cdot 10^9$ джонсів; зовнішньою квантовою ефективністю 0,8% та часом відгуку/відновлення у кілька хвилин. Він цілком підходить для портативних персональних пристроїв УФ моніторингу та як "електронне око" в системі безпеки дверей. Висока селективна чутливість пристрою до аміаку (NH_3) зумовлена синергетичним ефектом газу-донора електронів NH_3 на напівпровідник *p*-типу CuI та здатністю останнього до комплексоутворення з NH_3. Межа виявлення 0,15 ppm хемірезистивного сенсора аміаку CuI/ПЕ та його швидка реакція та швидке відновлення роблять його придатним для виявлення псування харчових продуктів, моніторингу витоків аміаку в режимі реального часу та медичної діагностики шляхом виявлення NH_3 у видихуваному повітрі.

Ключові слова: УФ детектори, хімічні детектори, гнучкі підкладинки, тонкі плівки, CuI, нанокристалічні шари.